http://dx.doi.org/10.5012/bkcs.2013.34.2.629

Anisotropy of the Electrical Conductivity of the Fayalite, Fe_2SiO_4, Investigated by Spin Dimer Analysis

Kee Hag Lee,[†,‡,*] Jeeyoung Lee,[‡] and Rüdiger Dieckmann[†]

[†]*Department of Materials Science and Engineering, Bard Hall, Cornell University, Ithaca, New York 14853-1501*
[‡]*Department of Chemistry, Nanoscale Science and Technology Institute, Wonkwang University, Iksan 570-749, Korea*
[*]*E-mail: khlee@wonkwang.ac.kr*
Received December 11, 2012, Accepted January 4, 2013

Many properties of inorganic compounds are sensitive to changes in the point-defect concentrations. In minerals, such changes are influenced by temperature, pressure, and chemical impurities. Olivines form an important class of minerals and are magnesium-rich solid solutions consisting of the orthosilicates forsterite Mg_2SiO_4 and the fayalite Fe_2SiO_4. Orthosilicates have an orthorhombic crystal structure and exhibit anisotropic electronic and ionic transport properties. We examined the anisotropy of the electrical conductivity of Fe_2SiO_4 under the assumption that the electronic conduction in Fe_2SiO_4 occurs *via* a small polaron hopping mechanism. The anisotropic electrical conductivity is well explained by the electron transfer integrals obtained from the spin dimer analysis based on tight-binding calculations. The latter analysis is expected to provide insight into the anisotropic electrical conductivities of other magnetic insulators of transition metal oxides.

Key Words : Fayalite, Fe_2SiO_4, Anisotropic electrical conductivity, Electron hopping, Spin dimer analysis

Introduction

In studying the structures, electronic and ionic transport properties, defect chemistry, and other mineral physical properties for most minerals, electrical conductivity measurements have been important because they are sensitive to subtle changes in defect chemistry. The properties of the olivine, $(Mg, Fe)_2SiO_4$, that constitutes one of the most abundant minerals in the Earth's upper mantle, are of considerable interest in geophysics and crystal chemistry.[1] The fayalite, Fe_2SiO_4, is the iron-rich end member of the olivine-type silicate and is important as ferrous component of the Mg-Fe-olivine solid solution series. The lattice of Fe_2SiO_4 has FeO_6 octahedra interwoven with SiO_4 tetrahedra. The olivine-type silicate Fe_2SiO_4 has an orthorhombic crystal structure, see Figure 1, with the space group *Pnma*, in which there are four formula units per unit cell.[2] Two crystallographically nonequivalent iron sites exist; Fe1 sites have inversion symmetry (S_2), and Fe2 sites mirror-plane symmetry (C_s).

Fe_2SiO_4 is a magnetic insulator with strong electron localization,[3] and its magnetic structure determined by Mössbauer spectroscopy and neutron-diffraction experiments on single crystal samples has a quite complex antiferromagnetic order below the Néel temperature 64.9 K.[4] The magnetic moments of the Fe2 sites are parallel to the *b* axis. The strong anisotropy in the measured magnetic susceptibility suggests strong correlations between the crystal structure and the electronic or magnetic properties. In fact, the imperfectly quenched orbital moments on the iron ions, which make their magnetic moments greater than their spin-only moments, allow spin-orbit coupling to produce the observed magnetocrystalline anisotropy.[4]

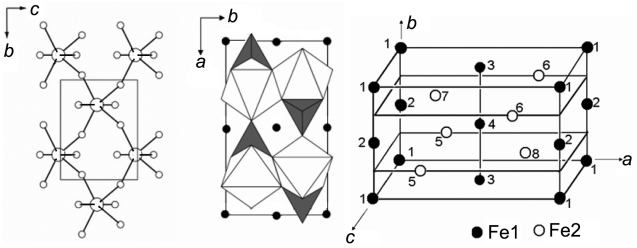

Figure 1. Crystal structure of olivine-type Fe_2SiO_4. (a) A perspective view of the FeO_2 layer made up of corner-sharing FeO_6 octahedra for Fe2 sites along the *a*-axis direction. (b) A projective view of how the FeO_2 layers stack of Fe2 sites along the *c*-axis direction. In panel (b), the SiO_4 units are indicated by shaded tetrahedra, the FeO_6 octahedra by unshaded octahedra for Fe2 sites, and the Fe1 sites by filled circles. (c) The positions of their magnetic sites in the chemical and magnetic unit cell. Here, the filled and unfilled circles represent Fe1 and Fe2 sites, respectively.

Fe_2SiO_4 shows anisotropic electrical conduction at high temperatures,[5,6] which is a relatively unexplored area.[7-10] Detailed measurements of the electrical conduction in the olivine[6] at high temperatures show that the replacement of significant quantities of Fe with Mg (about 10%) leads to hole localization on the Fe sites (small polarons) and charge hopping between Fe^{2+} and Fe^{3+}. Thus, the olivine is an electronic conductor over the geophysically interesting temperature range between ~1473 and ~1773 °K. The electrical conductivity is proportional to the charge mobility, which is in turn proportional to the square of the transfer integral. The high temperature conductivity means fast charge mobility because the activation energy for electron hopping over temperature can be readily overcome.

In recent years, the application of *ab initio* density functional theory (DFT) techniques for the study of minerals has expanded considerably and even detailed studies of the thermodynamic properties of some systems are available.[11] Quite recently, the structural, electronic, and magnetic properties of Fe_2SiO_4 were studied by using DFT with local-density approximation (LDA) and generalized gradient approximation (GGA).[12] However, these electronic structure calculations within the GGA predicted a metallic ground state, contrary to experimental evidence indicating a magnetic insulating behavior at ambient pressure and temperature.

In DFT calculations, the electronic structure of a magnetic insulator is not well described. DFT calculations with LDA or GGA often fail to produce a band gap for magnetic insulators. This deficiency of DFT calculations is often remedied by introducing an on-site repulsion (U) on magnetic ions.[13] Such DFT calculations are commonly referred to as LDA+U and GGA+U approaches.[14] Calculations using the GGA+U approach produced a more reasonable understanding of the electronic, magnetic, and optical properties of the fayalite, Fe_2SiO_4.[15] To the best of our knowledge, there is no theoretical study concerning the anisotropic electrical conductivity of the fayalite, Fe_2SiO_4, which we examine in the present work by performing spin dimer analyses based on extended Hückel tight-binding calculations. This tight-binding method provides a reliable means to determine the relative strengths of spin exchange interactions.[16] Here we investigate the hopping integrals between adjacent Fe sites, which should be enhanced to increase the charge mobility.

Theoretical Calculations

In insulators, the band gap is large (often 5 eV or more) and prevents thermal elevation of electrons into the valence band, and their charge transport occurs by ion movement (ionic conduction) or by electron hopping from one cation site to another (hopping conduction). Thus the electrical conductivity of a magnetic insulator is greatly influenced by point defects.[17] The electrical conduction of an insulator is thermally activated with energy barriers for the production and motion of charge carriers. At a given temperature T the electrical conductivity (σ) of a material is the sum of the conduction of each charge carrier acting in parallel.[18]

$$\sigma = \Sigma\, \sigma_i = \Sigma\, c_i\, q_i\, \mu_i \tag{1}$$

where c_i is the concentration of the charge carrier i [$c_i = c_{i0} \exp(-E_f/k_BT)$], q_i is its effective charge, and μ_i its mobility (in $m^2\ V^{-1}\ sec^{-1}$) [$\mu_i = \mu_{i0} \exp(-E_m/k_BT)$]. E_f and E_m are the activation energies of the formation and migration, and k_B is the Boltzmann's constant. In general, defects are present to some degree in every crystal and contribute to the total conductivity. In general, one or two types of defects dominate under a given set of thermodynamic conditions. The concentrations of the defect species are governed by chemical reactions leading to the production or removal of each defect type.

At high temperature when the motions of the carriers can be modeled by a sequence of uncorrelated hops, the key parameters defining the mobility are given by

$$\mu = (e\, a^2/k_BT)\, k_{ET}. \tag{2}$$

where e is the electron charge, a denotes the spacing between sites, and k_{ET} is the hopping probability per unit time (*i.e.*, the electron transfer rate). In a nonadiabatic electron transfer reaction, the vibrational motion is much faster than the electron motion so that the electronic wave function does not have enough time to move completely from the donor to the acceptor. Only a small fraction of the electron probability density can reach the donor state (tunneling). In this weak coupling limit, the electron transfer rate k_{ET} is proportional to t^2 (the square of the hopping integral between sites) and also depends on the probability with which the crossing region is reached by the vibrational coordinates (activation energy):[19,20]

$$k_{ET} \propto t^2 \exp(-E_{act}/k_BT). \tag{3}$$

Since the nonadiabatic limit is obtained when the coupling is very small, the splitting at the barrier top is very small and thermal fluctuations facilitate the electron transfer.[19-21]

In Fe_2SiO_4 under CO_2-CO atmospheres in the temperature range 1273-1423 °K, the possible predominant defect structure has been reported to be a disorder type of doubly ionized iron vacancies ($V''_{Fe,O}$) and an equivalent number of electron holes ($Fe^{\bullet}_{Fe,O}$). Here, $V''_{Fe,O}$ represents the vacancy of an iron ion on a regular site with octahedral coordination in the iron sublattice, and $Fe^{\bullet}_{Fe,O}$ the trivalent iron ion on a regular site with octahedral coordination in the iron sublattice. Moreover, the electrical conductivity of Fe_2SiO_4 is suggested to be driven by a small polaron mechanism.[7] This hopping model describes the transfer of a polaron (a localized electron with surrounding lattice deformation) and predicts a thermally activated diffusion process. The reported hopping model[6,7] supports the hypothesis that our spin dimer model[16] can be appropriate in interpreting the anisotropic electronic conductivity of the magnetic insulator Fe_2SiO_4.

In essence, electron localization is responsible for the insulating behavior of magnetic solids. Thus, we first consider the electronic structure of a dimer with one electron and one orbital per site to discuss the consequence of electron localization.[16] In addition, we examine its implications concerning the hopping integrals of general spin dimers. In the tight-binding approximation, the orbital energy difference Δe is related to the hopping integral t between the spin sites as

$$\Delta e = 2t \tag{4}$$

so that $t^2 \propto (\Delta e)^2$. If each spin site is represented by non-orthogonal orbitals φ_1 and φ_2 (instead of the orthogonal orbitals χ_1 and χ), the hopping integral t is proportional to the overlap integral S between them,[22] $t \propto S = \langle \varphi_1 | \varphi_2 \rangle$. Consequently, $t^2 \propto (\Delta e)^2 \propto S^2$.

Spin Dimer Approach. When 2 adjacent spin sites have M and N unpaired spins, respectively, the net spin orbital

interaction energy was discussed in terms of the sum of the spin-orbital interaction energy squares,[23-26]

$$<(\Delta\varepsilon)^2> = \frac{1}{MN}\sum_{\mu=1}^{M}\sum_{\nu=1}^{M}(\Delta\varepsilon_{\mu\nu})^2, \quad (5)$$

by calculating the $\Delta\varepsilon_{\mu\nu}$ values on the basis of fragment molecular orbital analysis. Here, the antiferromagnetic contribution of each term $\Delta\varepsilon_{\mu\nu}$ is zero when the non-orthogonal magnetic orbitals φ_μ and φ_ν are different in symmetry so that $S_{\mu\nu} = 0$; it is also negligible when φ_μ and φ_ν are different in shape so that $S_{\mu\nu}$ is negligibly small. Therefore, only the "diagonal" terms $\Delta\varepsilon_{\mu\nu}$ can contribute significantly in Eq. (5).[23-26] It should be noted that for SSE interactions the $<(\Delta\varepsilon)^2>$ value was discussed in terms of the sum of the electron transfer integrals ($t_{\mu\nu}$) as follows:

$$<(\Delta\varepsilon)^2> = \frac{1}{MN}\sum_{\mu=1}^{M}\sum_{\nu=1}^{M}(2t_{\mu\nu})^2. \quad (6)$$

where $t_{\mu\nu}$ represents the hopping integral between the magnetic orbitals φ_μ and φ_ν.

When two spin sites of a spin dimer consists of transition metal ions located at octahedral sites, each spin site can have three magnetic orbitals (φ_1, φ_2, φ_3) from the t_{2g}-block levels and two magnetic orbitals (φ_4, φ_5) from the e_g-block levels. For spin exchange interactions between spin sites containing different numbers of unpaired spins (M ≠ N) in terms of these magnetic orbitals, the following energy terms were defined:[23,24]

$$(\Delta\varepsilon_{t_{2g}})^2 = (\Delta\varepsilon_{11})^2 + (\Delta\varepsilon_{22})^2 + (\Delta\varepsilon_{33})^2,$$
$$(\Delta\varepsilon_{e_g})^2 = (\Delta\varepsilon_{44})^2 + (\Delta\varepsilon_{55})^2. \quad (7)$$

Then, the $<(\Delta\varepsilon)^2>$ value was approximated by

$$\langle(\Delta\varepsilon)^2\rangle \approx \frac{1}{MN}\left\{\frac{m_t}{3}\times\frac{n_t}{3}(\Delta\varepsilon_{t_{2g}})^2 + \frac{m_e}{2}\times\frac{n_e}{2}(\Delta\varepsilon_{e_g})^2\right\}. \quad (8)$$

when one spin site has m_t and m_e unpaired spins in the t_{2g}- and e_g-block levels, respectively ($M = m_t + m_e$), while the other spin site has n_t and n_e unpaired spins in the t_{2g}- and e_g-block levels, respectively ($N = n_t + n_e$). With regard to the fayalite Fe_2SiO_4 in the present work, $M = 4$ and $N = 5$ for Fe(II) and Fe(III) sites, respectively. The analysis given above can be extended in a similar manner to other cases of magnetic transition metal ions.[25] From the spin orbital interaction energy $\Delta\varepsilon_{\mu\mu}$ calculated for a spin dimer, the corresponding hopping integral can be estimated as $t_{\mu\mu} = \Delta\varepsilon_{\mu\mu}/2$. Since the effective on-site repulsion is nearly constant for a given system, the overall electron transfer integral (t) of the spin dimer can be written as $t_{12} \approx (<(\Delta\varepsilon)^2>/4)^{1/2}$. Therefore, the trends in the overall electron transfer integrals can be discussed in terms of the sum of the spin-orbital interaction energy squares.

Four Electron Transfer Integrals in Fe_2SiO_4. The electron transfer integrals are described by the parameters t_{ij}, many of which are equivalent because of the relationships such as $t_{15} = t_{38}$. Here, the subscripts refer to the site numbers of the magnetic ions involved in the electron transfer, which are shown in Figure 1(c). There are four independent transfer integrals to consider, namely, t_{12}, t_{15}, t_{35}, and t_{57}. The hopping integrals t_{57} and t_{35} are between the Fe atoms connected by corner-sharing FeO_6 octahedra, and the hopping integrals t_{12} and t_{15} between those connected by edge-sharing FeO_6 octahedra.

For a variety of magnetic solids, it has been found[16] that their magnetic properties are well described by the $<(\Delta\varepsilon)^2>$ values obtained from extended Hückel tight-binding calculations, when both the d orbitals of M and the s/p orbitals of its surrounding ligands are represented by double-ζ Slater-type orbitals.[27] The $<(\Delta\varepsilon)^2>$ values for the exchange interactions t_{12}, t_{15}, t_{35}, and t_{57} of Fe_2SiO_4 were calculated by employing the atomic orbital parameters of Table 1.[28]

In Fe_2SiO_4 the electron transfer (hopping) between adjacent Fe metal atoms occurs through M-L-M paths. In our spin dimer analysis, the hopping integrals are examined by performing electronic structure calculations for the spin dimers, *i.e.*, the structural units consisting of two Fe spin sites and their surrounding O atoms. The spin monomer containing a high-spin Fe^{2+} (d^6) ion is represented by the species $(FeO_6)^{10-}$ that has four magnetic orbitals, while that

Table 1. Exponents ζ and Valence Shell Ionization Potentials H_{ii} of Slater-Type Orbitals φ_i Used for Extended Hückel Tight-Binding Calculations[a]

Atom	φ_i	H_{ii} (eV)	ζ_1	C_1[b]	ζ_2	C_2[b]
Fe	4s	-9.10	1.925	1.0		
Fe	4p	-5.32	1.390	1.0		
Fe	3d	-12.6	6.068	0.4038	2.618	0.7198
O	2s	-32.3	2.688	0.7076	1.675	0.3745
O	2p	-14.8	3.694	0.3322	1.659	0.7448

[a] H_{ii}'s are the diagonal matrix elements $< \varphi_i \mid H_{\text{eff}} \mid \varphi_i >$, where H_{eff} is the effective Hamiltonian. In our calculations of the off-diagonal matrix elements $H_{\text{eff}} = < \varphi_i \mid H_{\text{eff}} \mid \varphi_j >$, the weighted formula was used.[29] [b] Coefficients used in the double-ζ Slater-type orbital expansion.

Table 2. Electron Transfer Integrals t_{ij} Values in meV and the Relative Ratio for the Electron Transfer Paths for [100], [010], and [001] Directions Calculated of Fe_2SiO_4

Paths	t_{12}	t_{15}	t_{57}	t_{35}	$t_{[100]}$[a]	$t_{[010]}$[a]	$t_{[001]}$[a]
Our work	31.85	6.50	21.46	9.00	0.08	1.0	0.31
Example of a single crystal Fe_2SiO_4 at 1403 K (converted from Fig. 5 in ref. 5)					0.50	1.0	0.93
Example of $(Mg, Fe)_2SiO_4$ San Carlos olivine at 1592 K (converted from Fig. 3 in ref. 6)					0.52	1.0	0.61

[a] Here, the $t_{[100]}$, $t_{[010]}$, and $t_{[001]}$ are obtained by using the series of electron-hopping paths in reference 30.

Table 3. Geometrical Parameters Associated with the Fe-O(edge-shared)-Fe and Fe-O(corner-shared)-Fe Paths of Fe_2SiO_4 fayalite[a]

Paths	t_{12}	t_{15}	t_{57}	t_{35}
M····M distance (Å)	3.075	3.340	3.973	3.650
∠M-O-M angle (°)	91.5, 91.2	99.0, 94.3	126.7	113.2

[a]Calculated from the crystal structure[2] at 1173 K (Smyth, J. R. *Am. Mineral*. **1975**, *60*, 1092).

containing a high-spin $Fe^{3+}(d^5)$) is represented by $(FeO_6)^{9-}$ with five magnetic orbitals. The spin dimers with a corner-sharing FeO_6 octahedra are given by $(Fe_2O_{11})^{17-}$, and those with an edge-sharing FeO_6 octahedra by $(Fe_2O_{10})^{15-}$. The relative values of t_{12}, t_{15}, t_{35}, and t_{57} obtained from the calculated $<(\Delta\varepsilon)^2>$ values are summarized in Table 2, and the geometrical parameters of these exchange paths in Table 3.

Table 2 reveals that the intralayer electron transfer integral t_{12} along the *b*-axis is stronger than the other interactions t_{15}, t_{35}, and t_{57}. The intralayer electron transfer integral interaction t_{57} in the bc-plane is the second strongest interaction. The interaction t_{15} is negligibly weaker than the t_{35} interaction. The Fe····Fe distances (Table 3) of the t_{ij} paths increase in the order $t_{12} < t_{15} < t_{35} < t_{57}$, so the short Fe····Fe distance does not necessarily guarantee that the associated Fe-O-Fe electron transfer integral is strong. Table 3 shows that the –Fe-O-Fe angles of the Fe-O(corner-shared)-Fe path are larger than those of the Fe-O(edge-shared)-Fe path. One might have supposed that the smaller –Fe-O-Fe angle leads to a weaker electron transfer integrals, but this is not the case because the different exchange paths do not refer to equivalent Fe sites.

Concluding Remarks

The anisotropic electrical conductivity of Fe_2SiO_4 is well explained by the electron transfer integrals of the four different spin exchange paths calculated by the spin dimer analysis based on tight-binding calculations. In particular, our results demonstrate that the orientation-dependent property of electron transfer integrals is important in understanding the anisotropic electrical conductivity of magnetic insulators.

Acknowledgments. This paper was supported by Wonkwang University in 2010. KHL thanks M.-H. Whangbo for invaluable discussion and comments.

References

1. Brown, G. E., Jr. *Olivines and Silicate Spinels*; In *Reviews in Mineralogy*, Ribbe, P. H., Ed.; Mineralogical Soc. Amer.: Washington, D. C., 1980; Vol. 5, Chap. 11.
2. (a) Smyth, J. R. *Am. Mineral*. **1975**, *60*, 1092. (b) Lottermoser, W.; Steiner, K.; Grodzicki, M.; Jiang, K.; Scharfetter, G.; Bats, J. W.; Redhammer, G.; Treutmam, W.; Hosoya, S.; Amthauer, G. *Phys. Chem. Minerals* **2002**, *29*, 112.
3. (a) Mao, H. K.; Bell, P. M. *Science* **1972**, *176*, 403. (b) Williams, Q.; Knittle, E.; Reichlin, R.; Martin, S.; Jeanloz, R. *J. Geophys. Res. B* **1990**, *95*(13), 21549.
4. Fuess, H.; Ballet, O.; Lottermoser, W. *Structural and Magnetic Phase Transitions in Minerals*. In *Advances in Physical Geochemistry*, Ghose, S., Coey, J. M. D., Salje, E., Eds.; Springer-Verlag: Berlin, 1988; Vol. 7, p 185.
5. Tsai, T.-L.; Dieckmann, R. *Materials Science Forum* **1997**, *239*, 399.
6. Schock, R. N.; Duba, A. G.; Shankland, T. J. *J. Geophys. Res.* **1989**, *94*, 5829.
7. Sockel, H. G. *Defect Structure and Electrical Conductivity of Crystalline Ferrous Silicate*; In *Defects and Transport in Oxide*; Seltzer, M. S.; Jaffee, R. I., Eds.; Prenum Press: New York, 1974; pp 341-356.
8. Schock, R. N.; Duba, A. C. In *Point Defects and the Mechanisms of Electrical Conduction in Olivine*; Shock, R. N., Ed.; Amer. Geophys. Union: Washington, D. C., 1985; pp 88-96.
9. Hirsch, L. M.; Shankland, T. J.; Duba, A. G. *Geophys. J. Int.* **1993**, *114*, 36.
10. Constable, S.; Roberts, J. J. *Phys. Chem. Minerals* **1997**, *24*, 319.
11. Brodholt, J. P.; Voèadlo, L. *MRS Bulletin* **2006**, *31*, 675 and references therein. Hafner, J.; Wolverton, C.; Ceder, G. *MRS Bulletin* **2006**, *31*, 659 and references therein.
12. Cococcioni, M.; Corso, A. D.; de Gironcoli, S. *Phys. Rev. B* **2003**, *67*, 094106.
13. Mott, N. F. *Metal-Insulator Transitions*; Taylor and Frances: London, 1974; Mott, N. F. *Metal-Insulator Transitions*, 2nd ed.; Taylor & Francis: New York, 1990.
14. Anisimov, V. I.; Zaanen, J.; Andersen, O. K. *Phys. Rev. B* **1991**, *44*, 943.
15. Jiang, X.; Guo, G. Y. *Phys. Rev. B* **2004**, *69*, 155108.
16. Whangbo, M.-H.; Koo, H.-J.; Dai, D. *J. Solid State Chem.* **2003**, *176*, 417 and references therein.
17. Kroger, F. A. *The Chemistry of Imperfect Crystals*; North-Holland Pub. Co.: Amsterdam, 1974.
18. Tyburczy, J. A.; Fisler, D. K. *Electrical Properties of Minerals and Melts*; In *Mineral Physics and Crystallography, A Handbook of Physical Constants*; Amer. Geophys. Union: Washington, D. C., 1995; pp 185-208.
19. Coropceanu, V.; André, J. M.; Malagori, M.; Brédas, J. L. *Theo. Chem. Acc.* **2003**, *110*, 59.
20. Newton, M. D. *Electron Transfer: Theoretical Models and Computational Implementation,* In *Electron Transfer in Chemistry*; Balzani, V., Ed.; Wiley-VCH: New York, 2001; Chap. 1.
21. Marcus, R. A. *Rev. Mod. Phys.* **1993**, *65*, 599.
22. Albright, T. A.; Burdett, J. K.; Whangbo, M.-H. *Orbital Interactions in Chemistry*; Wiley: New York, 198; Chapter 2.
23. Koo, H.-J.; Whangbo, M.-H.; Coste, S.; Jobic, S. *J. Solid State Chem.* **2001**, *156*, 464.
24. Dai, D.; Koo, H.-J.; Whangbo, M.-H. In *MRS Symposium Proceedings, Vol. 658*; Geselbracht, M. J., Greedan, J. E., Johnson, D. C., Subramanian, M. A., Eds.; Materials Research Society: Warrendale, PA, 2001; GG5.3.1-5.3.11.
25. Whangbo, M.-H.; Koo, H.-J.; Dai, D.; Jung, D. *Inorg. Chem.* **2002**, *41*, 5575.
26. Whangbo, M.-H.; Koo, H.-J.; Dumas, J.; Continentino, M. A. *Inorg. Chem.* **2002**, *41*, 2193.
27. Clementi, E.; Roetti, C. *Atomic Data Nuclear Data Tables* **1974**, *14*, 177.
28. Our calculations were carried out by employing the SAMOA (Structure and Molecular Orbital Analyzer) program package (Dai, D.; Ren, J.; Liang, W.; Whangbo, M.-H. http://chvamw.chem.ncsu.edu/, 2002).
29. Ammeter, J.; Bürgi, H.-B.; Thibeault, J.; Hoffmann, R. *J. Am. Chem. Soc.* **1978**, *100*, 3686.
30. Lee, K. H.; Dieckmann, R.; Lee, C.; Whangbo, M.-H. *Chem. Mater.* **2007**, *19*, 4393.